Journal of Catalysis 340 (2016) 344–353

Contents lists available at ScienceDirect

Journal of Catalysis

journal homepage: www.elsevier.com/locate/jcat

Heterogenization of chiral mono oxazoline ligands by grafting onto mesoporous silica MCM-41 and their application in copper-catalyzed asymmetric allylic oxidation of cyclic olefins

Saadi Samadi [a,*], Khosrow Jadidi [b,*], Behnam Khanmohammadi [b], Niloofar Tavakoli [b]

[a] Laboratory of Asymmetric Synthesis, Department of Chemistry, Faculty of Science, University of Kurdistan, 66177-15175 Sanandaj, Iran
[b] Department of Chemistry, Shahid Beheshti University, G.C., Tehran 1983963113, Iran

ARTICLE INFO

Article history:
Received 6 April 2016
Revised 19 May 2016
Accepted 23 May 2016

Keywords:
Chiral recyclable heterogeneous catalysts
Chiral mono oxazoline ligands
Mesoporous MCM-41
Asymmetric allylic oxidation

ABSTRACT

A series of chiral 4-oxazolinylaniline ligands **8** were conveniently synthesized on a gram scale from inexpensive and commercially available 4-aminobenzoic acid in four steps. The obtained organic chiral ligands have been covalently grafted onto ordered mesoporous silicas MCM-41 and the resulting inorganic–organic hybrid materials have been characterized by thermogravimetric analysis (TGA), differential thermal analysis (DTA), powder X-ray diffraction, BET and BJH nitrogen adsorption–desorption methods, energy-dispersive X-ray spectroscopy (EDX), CHN analysis, scanning electron microscopy (SEM), and Fourier transform infrared spectroscopy (FT-IR). The catalytic and induced asymmetric effects of the chiral copper (I) complexes of these new chiral supported heterogeneous catalysts on the asymmetric allylic oxidation of cycloolefins were investigated under different conditions. Reactions using the catalyst exhibited moderate to good enantioselectivities, up to 80%, and good yields, up to 95% better than the corresponding homogeneous reaction. The catalyst could be recovered easily and reused five times without remarkable loss of reactivity, yield, or enantioselectivity. This is, to the best of our knowledge, the first heterogenization of chiral 4-oxazolinylaniline ligands on an inorganic (silica) surface and their application as a heterogeneous catalyst in the asymmetric Kharash–Sosnovsky reaction.

1. Introduction

In recent years, many researchers have taken great interest in the heterogenizing of homogeneous catalysts, which is mainly due to the practical advantages of easy separation of catalysts and products by simple filtration and reuse of expensive chiral catalysts. One of the main drawbacks of heterogeneous catalysts is their often reduced activity relative to their homogeneous counterparts [1–4], although some contrary cases have been reported [5,6]. These phenomena have been related to the local density of the catalysts on the heterogeneous material, to accessibility of the catalysts on the materials, and to various interactions with functional groups of the materials [3].

Inorganic solids are of great importance, especially since the discovery of a new class of mesoporous molecular sieves such as MCM and SBA containing reactive silanol groups, which offer large pores and high surface area to the guest ligand–metal complex with considerable stability under different reaction conditions [7–13].

Among different immobilization techniques, the formation of covalent bonds between the support and the chiral ligand is the most common strategy, which is to be more resistant toward leaching during catalytic reactions, which may improve catalyst recycling.

Chiral oxazoline ligands are a class of nitrogen ligands that have been successfully used in the asymmetric catalysis of a variety of reactions for the past decade [14–16]. These chiral ligands offer the advantage that they are in general less structurally complex than bis- and trisoxazoline ligands and are readily achieved in a few steps from amino alcohols [17–19]. Although there is wide application of chiral bisoxazoline ligands in catalytic asymmetric synthesis, mono oxazoline versions have rarely had the same impact, but some examples show that mono oxazoline gave better enantioselectivity than bisoxazoline. However, these versatile catalytic systems suffer from one major drawback: a high catalyst-to-substrate ratio is required (generally 1–10 mol%) and their separation and recycling is therefore a prerequisite for their development as useful catalysts. Regarding the preparation of multipurpose catalysts and for the above-mentioned reasons, mono

* Corresponding authors.

http://dx.doi.org/10.1016/j.jcat.2016.05.021
0021-9517/

oxazoline ligands appear to be suitable candidates to heterogenize [20–22].

In 2013 our groups reported for the first time the use of nanoparticles and nanoporous materials as additives in the presence of biaryl bisoxazoline in the asymmetric allylic oxidation of cycloolefins [14–16]. The results showed that these materials have a participatory role in increasing the efficiency of the reaction. The intense effect of these additives in this reaction encouraged us to investigate the heterogenization of chiral 4-oxazolinylaniline ligands on mesoporous MCM-41.

The allylic oxidation of olefins using peresters in the presence of copper catalysts to give allylic esters is known as the Kharash–Sosnovsky reaction. This reaction has been the subject of great interest over the past decade and provides access to chiral allylic alcohols, which are key intermediates in natural product synthesis [23–29]. In this paper, we report the preparation and characterization of the chiral heterogeneous catalyst OX-R-MCM-41 as a novel chiral oxazoline-based solid catalyst and employ copper complexes of OX-R-MCM-41 in the enantioselective Kharash–Sosnovsky reaction.

2. Experimental

2.1. Materials and characterization methods

Melting points were measured on an Electrothermal 9100 apparatus and are uncorrected. Optical rotations were measured with a Perkin–Elmer 341 polarimeter at 589 nm. ^{1}H and ^{13}C NMR spectra were recorded on a BRUKER DRX-300 AVANCE spectrometer at 300.13 and 75.47 MHz, 62.5 MHz in $CDCl_3$ and DMSO-d_6 using TMS (δ = 0.0 ppm) as internal standard. IR spectra were recorded on a Bomen FT-IR-MB-series instrument. TGA–DTA analysis was carried out from 10 to 800 °C at a heating rate of 10 °C/min in air using a STA 503 M system from Bähr GmbH, Germany. X-ray diffraction patterns were obtained on a STOE diffractometer with Cu Kα radiation. Electron microscopy was performed on a TESCAN WEGAM scanning electron microscope (SEM). The enantiomeric excess (ee) of the products was determined by HPLC analysis using an EC 250/4.6 Nucleocel Alpha S column. All reactions were performed under dry, oxygen-free nitrogen. All reagents and starting materials were purchased from Aldrich, Merck, Fluka, and Sigma. Olefins were distilled from calcium hydride before use. All solvents for the reactions were of reagent grade and were dried and distilled immediately before use, as follows: acetonitrile and acetone from P_2O_5, methylene chloride from calcium hydride. Column chromatography was performed using silica gel 60 (230 ± 400 mesh) eluted with ethyl acetate and *n*-hexane. TLC was performed using silica gel 60 F_{256} plates with visualization by UV.

2.2. Preparation of the chiral mono oxazoline ligands **8a–8d**

The preparation of the chiral 4-oxazolinylaniline ligands is outlined in Scheme 1.

2.2.1. Typical procedure for the synthesis of hydroxy amides **6a–6d**

To a solution of 4-((*tert*-butoxycarbonyl)amino)benzoic acid **2** [30] (S2 in the Supplementary Material) (0.71 g, 3.0 mmol) in 10 ml of anhydrous methylene chloride were added 0.62 ml (6 mmol) of oxalyl chloride and then DMF (2 drops) at 0 °C. The reaction mixture was stirred for 4 h at 0 °C under N_2. The solvent was removed under reduced pressure to afford the acid chloride as a light yellow solid (0.77 g, 99%). This solid residue was then dissolved in 10 ml of anhydrous methylene chloride, cooled to 0 °C, and slowly added to a stirred solution of (*S*)-phenyl glycinol **5a** (0.45 g, 3.2 mmol) [31] and triethylamine (0.5 ml, 3.6 mmol) in 10 ml anhydrous methylene chloride at 0 °C. The reaction mixture was allowed to warm to room temperature slowly and stirred overnight under nitrogen. TLC analysis of the reaction (50:50 EtOAc/*n*-hexane) confirmed the formation of the new compound **6a**. After completion of the reaction, brine (10 ml) was added and the aqueous layer was extracted with ethyl acetate (3 × 5 ml) and dried over magnesium sulfate, filtered, and concentrated. Product **6a** was separated by flash chromatography (20–50% EtOAc/*n*-hexane) as a white solid with 86% total yield. Compounds **6b–6d** were synthesized by a similar method. The total yields for **6b**, **6c**, and **6d** were 90%, 85%, and 92%, respectively [14].

(S)-tert-butyl (4-((2-hydroxy-1-phenylethyl)carbamoyl)phenyl)carbamate (**6a**): Mp: 194–197 °C, ^{1}H NMR (300 MHz, $CDCl_3$): δ_H (ppm) = 1.54 (9H, s), 4.00–4.04 (2H, m), 5.25–5.30 (1H, m), 6.68 (1H, s, NH), 6.78–6.80 (1H, d, *J* = 6.5 Hz, NH), 7.30–7.40 (5H, m,

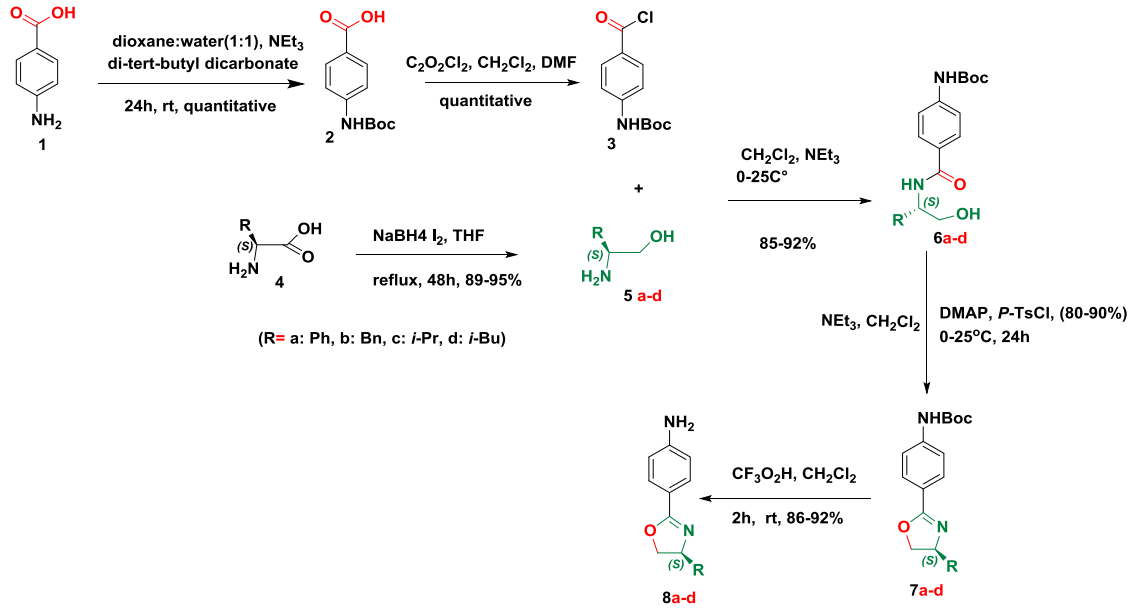

Scheme 1. Synthesis of chiral 4-oxazolinyl aniline ligands **8a–8d**.

Ar), 7.43–7.46 (2H, d, J = 8.5 Hz), 7.76–7.79 (2H, d, J = 8.5 Hz); ^{13}C NMR (75 MHz, DMSO-d_6): δ_C (ppm) = 28.5, 56.3, 64.9, 80.0, 117.4, 127.3, 127.4, 128.5,128.7, 128.9, 141.9, 142.7, 143.8, 153.1, 166.2. IR (KBr, cm^{-1}): 1516, 1630, 1704, 2632, 2977, 3355.

(S)-tert-butyl (4-((1-hydroxy-3-phenylpropan-2-yl)carbamoyl) phenyl)carbamate (**6b**): Mp: 167–170 °C, ^{1}H NMR (300 MHz, $CDCl_3$): δ_H (ppm) = 1.53 (9H, s), 2.98–3.00 (2H, brd, J = 6.8 Hz), 3.66–3.72 (1H, dd, J = 10.9, 5.2 Hz), 3.77–3.82 (1H, dd, J = 10.9, 3.0 Hz), 4.34 (1H, m), 6.38–6.40 (2H, brd, J = 7.1 Hz, NH), 6.74 (1H, s, NH), 7.25–7.32 (5H, m, Ar), 7.37–7.40 (2H, d, J = 8.4 Hz), 7.59–7.62 (2H, d, J = 8.4 Hz); ^{13}C NMR (75 MHz, $CDCl_3$): δ_C (ppm) = 28.3, 37.0, 53.4, 64.4, 81.1, 117.7, 126.8, 128.1, 128.3, 128.8, 129.3, 137.6, 141.6, 152.3, 167.6; IR (KBr, cm^{-1}): 1513, 1627, 1698, 2634, 2979 3355; MS m/z (%): 370 (M, 6), 279 (36), 220 (57), 164 (93), 120 (72), 91 (57), 57 (100).

(S)-tert-butyl(4-((1-hydroxy-3-methylbutan-2-yl)carbamoyl) phenyl)carbamate (**6c**): Mp: 157–160 °C, ^{1}H NMR (300 MHz, $CDCl_3$): δ_H (ppm) = 1.02–1.06 (6H, t, J = 6.1 Hz), 1.54 (9H, s), 2.00–2.06 (1H, m), 3.81 (2H, brs), 3.94 (1H, brs), 6.29–6.31 (1H, brd, J = 7.2 Hz, NH), 6.7 (1H, s, NH), 7.43–7.46 (2H, d, J = 7.9 Hz), 7.72–7.75 (2H, d, J = 8 Hz). ^{13}C NMR (75 MHz, $CDCl_3$): δ_C (ppm) = 19.1, 19.7, 28.3, 29.3, 57.6, 64.1, 81.2, 117.8, 128.4, 128.6, 141.6, 152.2, 167.9; IR (KBr, cm^{-1}): 1513, 1619, 1699, 2656, 2983, 3343.

(S)-tert-butyl(4-((1-hydroxy-4-methylpentan-2-yl)carbamoyl) phenyl)carbamate (**6d**): Mp: 150–152 °C, ^{1}H NMR (300 MHz, $CDCl_3$): δ_H (ppm) = 0.95 (3H, brs), 0.97 (3H, brs), 1.2–1.31 (1H, m), 1.53 (9H, s), 1.63–1.72 (2H, m), 3.60–3.65 (1H, dd, J = 10.6, 5.6 Hz), 3.74–3.79 (1H, dd, J = 10.6, 3.0 Hz), 4.244.25 (1H, m), 6.34 (1H, d, J = 8.0 Hz, NH), 6.87 (1H, s, NH), 7.39–7.42 (2H, d, J = 8.3 Hz), 7.68–7.71 (1H, d, J = 8.3). ^{13}C NMR (75 MHz, $CDCl_3$): δ_C (ppm) = 22.3, 23.1, 25.0, 28.3, 40.3, 50.4, 66.2, 81.1, 117.8, 128.1, 128.3, 141.6, 152.4, 167.7; IR (KBr, cm^{-1}): 1516, 1635, 1710, 2860, 2957, 3445.

2.2.2. Typical procedure for the synthesis of compounds **7a–7d**

A flame-dried round-bottom flask with a stirrer bar was charged with white hydroxy amid **6a** (3.5 mmol, 1.1 g, 1 equiv), 4-(dimethylamino) pyridine (0.02 g, 0.18, 0.1 equiv) and CH_2Cl_2 (10 ml) under N_2. Triethylamine (1.1, 7.7 mmol, 2.2 equiv) was added to mixture of reaction. The flask was placed in ice, and a solution of *p*-toluenesulfonyl chloride (0.67 g, 3.5 mmol, 2 equiv) in 4 ml of CH_2Cl_2 was added. The light yellow clear solution was stirred at room temperature for 12 h. The reaction mixture was diluted with 10 ml of CH_2Cl_2, and upon washing with 10 ml of saturated aqueous NH_4Cl, two layers were separated, and the aqueous layer was extracted again with CH_2Cl_2 (2 × 5 ml). The combined organic extracts were washed with 10 ml of saturated aqueous $NaHCO_3$, the organic layer was dried over Na_2SO_4, and a concentrated, light yellow oil was achieved and purified by column chromatography (25–75% EtOAc/*n*-hexane) to afford a pure light yellow product **7a** in 85% yield. Compounds **7b–7d** were synthesized by a similar method. The total yields were 85%, 80%, and 95%, respectively [14–16].

(S)-tert-butyl (4-(4-phenyl-4,5-dihydrooxazol-2-yl)phenyl)carbamate (**7a**): ^{1}H NMR (300 MHz, $CDCl_3$): δ_H (ppm) = 1.54 (9H, s), 4.24–4.30 (1H, t, J = 8.2 Hz), 4.76–4.82 (1H, t, J = 9.2 Hz), 5.34–5.40 (1H, dd, J = 8.4, 9.7 Hz), 6.83 (1H, s, NH), 7.328–7.36 (5H, m, Ar), 7.44–7.47 (2H, d, J = 8.6 Hz), 7.96–7.99 (2H, d, J = 8.6 Hz); ^{13}C NMR (75 MHz, DMSO-d_6): δ_C (ppm) = 28.5, 56.3, 65.0, 79.9, 117.5, 127.4, 128.5, 128.7, 139.1, 142.0, 142.7, 153.1, 166.1; IR (KBr, cm^{-1}): 1516, 1630, 1710, 2920, 2977, 3357

(S)-tert-butyl (4-(4-benzyl-4,5-dihydrooxazol-2-yl)phenyl)carbamate (**7b**): ^{1}H NMR (300 MHz, $CDCl_3$): δ_H (ppm) = 1.54 (9H, s), 2.71–2.79 (1H dd, J = 13.5, 9.0 Hz), 3.23–3.30 (1H, dd, J = 13.7, 4.7 Hz), 4.13–4.18 (1H, t, J = 7.6 Hz), 4.32–4.38 (1H, t, J = 8.8 Hz), 4.54–4.64 (1H m), 6.68 (1H s, NH), 7.25–7.34 (5H m, Ar), 7.42–7.45 (2H, d, J = 8.3 Hz), 7.89–7.92 (2H d, J = 8.4 Hz); IR (KBr, cm^{-1}): 1516, 1638, 1724, 2920, 2979, 3360; MS m/z (%): 353 (M, 100), 297 (73), 261 (42), 205 (62), 161 (33), 91 (27), 57 (61).

(S)-tert-butyl (4-(4-isopropyl-4,5-dihydrooxazol-2-yl)phenyl)carbamate (**7c**): ^{1}H NMR (300 MHz, $CDCl_3$): δ_H (ppm) = 0.83–0.86 (3H, d, J = 6.7 Hz), 0.93–0.95 (3H, d, J = 6.6 Hz), 1.41 (9H, s), 1.78–1.80 (1H, m), 4.04–4.08 (1H, m), 4.31 (1H, m), 4.81 (1H, brs), 7.39–7.82 (5H, m); IR (KBr, cm^{-1}): 1528, 1638, 1704, 2925, 2974, 3363.

(S)-tert-butyl (4-(4-isobutyl-4,5-dihydrooxazol-2-yl)phenyl)carbamate (**7d**): ^{1}H NMR (300 MHz, $CDCl_3$): δ_H (ppm) = 0.93–0.97 (6H, m), 1.25 (9H, s), 1.32–1.39 (1H, m), 1.64–1.81 (2H, m), 3.89–3.94 (1H, m), 4.20–4.31 (1H, m), 4.40–4.46 (1H, m), 6.60–6.62 (2H, brd, J = 8.7 Hz), 7.70–7.72 (2H, brd, J = 8.6 Hz). ^{13}C NMR (75 MHz, $CDCl_3$): δ_C (ppm) = 22.7, 23.0, 25.5, 29.4, 45.7,53.4, 64.8, 72.8, 114.1, 117.5, 129.8, 149.4, 163.5; IR (KBr, cm^{-1}): 1516, 1633, 2917, 2957, 3426.

2.2.3. Typical procedure for the synthesis of 4-oxazolinylaniline ligands **8a–8d**

A portion of 2.8 mmol (1 g) of (*S*)-*tert*-butyl (4-(4-phenyl-4,5-dihydrooxazol-2-yl)phenyl) carbamate **7a** was placed in a round-bottom flask (25 ml) containing 6:1 dichloromethane:trifluoroacetic acid (9 ml). The reaction solution was stirred for 3 h at room temperature. After completion of the reaction (as determined by TLC analysis), 10 ml of water was added. The organic layer was washed with 10 ml of aqueous sodium hydrogen carbonate (5%) and then dried over Na_2SO_4 to yield a concentrated light yellow oil. Purification using flash chromatography (30–40% EtOAc/*n*-hexane) afforded a light yellow product **8a** in 85% yield. Compounds **8b–8d** were synthesized by a similar method. The yields for other products were 84%, 93%, and 86%, respectively [30].

(S)-4-(4-phenyl-4,5-dihydrooxazol-2-yl)aniline (**8a**): ^{1}H NMR (300 MHz, $CDCl_3$): δ_H (ppm) = 4.21–4.26 (1H, t, J = 8.0 Hz), 4.73–4.79 (1H, t, J = 9.1 Hz), 5.32–5.38 (1H, m), 6.68–6.71 (2H, d, J = 8.0 Hz), 7.28–7.36 (5H, m, Ar), 7.84–7087 (2H, d, J = 8.1 Hz); ^{13}C NMR (75 MHz, DMSO-d_6): δ_C (ppm) = 69.9, 74.7, 113.8, 126.8, 128.7, 130.2, 131.7, 142.8, 149.8, 151.3, 166.5; MS m/z (%): 239 (M + 1, 100), 208 (75), 180 (20), 120 (63), 89 (30), 65 (23); $[\alpha]_{20}^{D}$ = +40.3° (*c* 1.0, CH_2Cl_2).

(S)-4-(4-benzyl-4,5-dihydrooxazol-2-yl)aniline (**8b**): ^{1}H NMR (300 MHz, $CDCl_3$): δ_H (ppm) = 2.94–3.02 (1H, m), 3.22–3027 (1H, m), 4.60–4.82 (3H, m), 6.60–6.63 (2H, d, J = 8.5 Hz), 7.19–7.34 (5H, m), 7.75–7.81 (2H, d, J = 8.8 Hz); ^{13}C NMR (75 MHz, $CDCl_3$): δ_C (ppm) = 34.8, 70.3, 73.1, 109.9, 123.3, 124.8, 125.2, 128.7, 129.8, 131.8, 141.3, 151.3, 166.1; MS m/z (%): 253 (12.5, M + 1), 216 (11.25), 179 (79.7), 161 (93.8), 133 (37.5), 120 (100), 106 (31.3), 91 (76.5), 65 (51.3); $[\alpha]_{20}^{D}$ = +10.7° (*c* 1.0, CH_2Cl_2).

(S)-4-(4-isopropyl-4,5-dihydrooxazol-2-yl)aniline (**8c**): ^{1}H NMR (300 MHz, $CDCl_3$): δ_H (ppm) = 0.97–0.99 (3H, d, J = 6.7 Hz), 1.03–1.1 (3H, d, J = 6.7 Hz), 2.05–2.11 (1H, m), 4.37–4.42 (1H, m), 4.47–4.53 (1H, m), 4.68–4.75 (1H, m), 6.67–6.70 (2H, d, J = 8.5 Hz), 7.93–7.95 (2H, d, J = 8.5 Hz). ^{13}C NMR (75 MHz, $CDCl_3$): δ_C (ppm) = 12.8, 13.8, 25.4, 67.8, 110.0, 127.8, 128.1, 143.4, 148.9 MS m/z (%): 204 (23.1, M), 179 (9.6), 161 (100), 133 (55.8), 120 (86.5), 106 (57.7), 92 (28.8), 85.2 (19.2), 77 (40.4), 72 (75). $[\alpha]_{20}^{D}$ = +27.6° (*c* 1.0, CH_2Cl_2).

(S)-4-(4-isobutyl-4,5-dihydrooxazol-2-yl)aniline (**8d**): ^{1}H NMR (300 MHz, $CDCl_3$): δ_H (ppm) = 0.96–0.99 (6H, m), 1.48–1.58 (1H, m), 1.77–1.91 (2H, m), 4.48–4.63 (2H, m), 4.93–5.10 (1H, m), 6.65–6.67 (2H, d, J = 8.5 Hz), 7.90–7.92 (2H, d, J = 8.5 Hz). MS m/z (%): 218 (M, 2.5), 203 (1), 161 (25), 120 (44), 85 (64), 71 (97), 57 (100). $[\alpha]_{20}^{D}$ = +14.3° (*c* 1.0, CH_2Cl_2).

2.3. Preparation of the chiral heterogeneous catalysts **9**

The preparation of the chiral heterogeneous catalysts **9** is outlined in Scheme 2.

The MCM-41 and Cl-MCM-41 mesoporous silicas were synthesized according to previously reported procedures [32,33] (S43 in the Supplementary Material).

A flame-dried 100 ml Schlenk flask equipped with a stirrer bar was charged with 2 g of modified support Cl-MCM-41 and 20 ml of anhydrous toluene under nitrogen. A stirred solution of (*S*)-4-(4-phenyl-4,5-dihydrooxazol-2-yl)aniline **8a** (5 mmol, 0.95 g) and triethylamine (1 ml) in anhydrous toluene (20 ml) was added slowly to the reaction mixture. The solution was allowed to warm and reflux with stirring overnight under N_2. The modified nonporous (Ox-Ph-MCM-41) was collected by filtration and washed thoroughly with CH_2Cl_2/CH_3OH. Then it was Soxhlet extracted with CH_2Cl_2/CH_3OH (1:1) for 24 h to remove any untethered species, and the light gray solid was dried at room temperature [32,33].

2.4. Enantioselective allylic oxidation of cycloolefins

Enantioselective allylic oxidation of cycloolefins is outlined in Scheme 3.

The chiral heterogonous catalyst **9a** was dried under vacuum at 40 °C for 4 h prior to use. To a flame-dried round-bottom flask (25 ml), the required amounts of dried chiral heterogeneous catalyst **9a** (100 mg), copper salt (0.55 mmol, 20 mg), and anhydrous CH_3CN (4 ml) were added and stirred for 3 h at ambient temperature under N_2. To this solution was added phenylhydrazine (6 μl, 0.06 mmol) with stirring. The color of the solution changed from blue green to red. Next cycloolefin (5 mmol) was added. The reaction mixture was cooled to −10 °C and then *tert*-butyl *p*-nitrobenzoperoxoate (0.203 g, 0.85 mmol) (S63 in the Supplementary Material) was added dropwise to the reaction solution under nitrogen. The mixture was kept at −10 °C until TLC showed to complete disappearance of perester. The chiral heterogeneous catalyst **9a** was collected by filtration and then thoroughly washed with methylene chloride (3 × 8 ml) and air-dried. Chiral catalysts were reused under the same conditions. After filtration the dichloromethane phase was washed with saturated aqueous NH_4Cl (10 ml). The extracted organic layers were combined and washed with saturated aqueous $NaHCO_3$ (10 ml), dried over $MgSO_4$, and concentrated. The crude residue obtained was purified by flash chromatography (2–10% EtOAc/*n*-hexanes) to yield a white solid **11**–**15** with up to 95% yield (S63–S8 in the Supplementary Material) [14].

3. Results and discussion

3.1. Synthesis of chiral 4-oxazolinylaniline ligands ***8a–8d***

Synthesis of chiral mono oxazoline ligands **8** can be performed with excellent yields and enantiomeric excess from the inexpensive starting material 4-aminobenzoic acid **1** (Scheme 1). The synthesis starts with production of Boc-protected intermediate **2** by the reaction of di-*tert*-butyl dicarbonate and triethylamine in aqueous dioxane in high yield [30]. Next, 4-((*tert*-butoxycarbonyl) amino) benzoic acid **2** was converted to acid chloride **3** by oxalyl chloride reagent in the presence of a catalytic amount of DMF at 0 °C. The hydroxy amides **6a**–**6d** were obtained after treatment of acid chloride **3** with four individual *S*-amino alcohols **5a**–**5d** [31] at 0 °C. To achieve the best procedure for the synthesis of the desired ligand **8**, we required an efficient method for cyclization of the hydroxyamides' precursor **6a**–**6d**. For this purpose, we tested several methods, and in the best procedure, compounds **7a**–**7d** were prepared at high yield by stirring the mixture of the hydroxyamides **6a**–**6d** overnight in the presence of *p*-TsCl, DAMP, and Et_3N at room temperature. In the final step, chiral 4-oxazolinyl aniline ligands **8a**–**8d** were achieved by removing the protective group from **7a** to **7d** in the presence of trifluoroacetic acid in methylene chloride (14% TFA/DCM) (Scheme 1) [14,30].

3.2. Synthesis of the chiral heterogeneous catalyst OX-R-MCM-41 ***9a–9d***

For preparation of the chiral heterogeneous catalyst, MCM-41 was prepared and characterized according to the literature. The surface hydroxyl groups of MCM-41 were first reacted with the methoxy groups of 3-chloropropyltriethoxysilane. In this grafting reaction, two main methoxy groups of the silylating agent were replaced with silanol groups of the surface [33–36]. The chloropropyl groups were then reacted with amino groups of chiral 4-oxazolinyl aniline ligands **8a**–**8d** to yield new supported heterogeneous catalysts OX-R-MCM-41 **9** (Scheme 2).

3.3. Characterization of the chiral catalyst OX-R-MCM-41 ***9a–9d***

Due to the insolubility of OX-R-MCM-41 in all common organic solvents, its structural investigation was limited to its physicochemical properties, thermogravimetric analysis (TGA), differential thermal analysis (DTA), BET and BJH nitrogen adsorption–desorption methods, scanning electron microscopy (SEM), powder X-ray

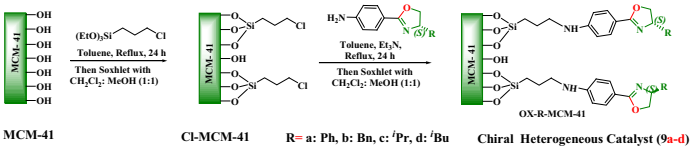

Scheme 2. Synthesis of chiral heterogeneous catalysts OX-R-MCM-41 **9a**–**9d**.

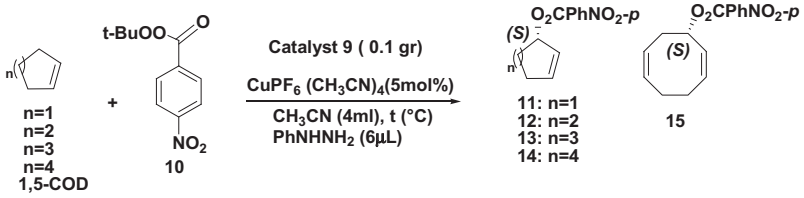

Scheme 3. Allylic oxidation of cycloolefins in the presence of a chiral catalyst (OX-R-MCM-41).

diffraction, energy-dispersive X-ray spectroscopy (EDX), CHN analysis, and Fourier transform infrared (FT-IR) spectral data.

3.3.1. Spectroscopic characterization and thermogravimetric analysis

The FT-IR spectra of Cl-MCM-41 confirmed the presence of organosilane and chlorine groups on the surfaces of the mesoporous silicas with characteristic peaks (3444, 2928, and 699 cm^{-1}) and clearly demonstrated that the mesoporous structure of MCM-41 was preserved after modification. In the FT-IR spectrum of the chiral catalyst OX-R-MCM-41, the characteristic band at 1000–1250 cm^{-1} is due to the Si—O stretching in the Si—O—Si structure. The spectra showed a broad band around 3200–3680 cm^{-1}, which is due to adsorbed water molecules. The presence of asymmetric vibration in the range 1656–1708 cm^{-1} for C=N confirmed the presence of the oxazoline group (Table 1). OX-R-MCM-41 showed the characteristic asymmetric vibration of the CH_2 groups of the propyl chain of the silylating agent at around 2958 cm^{-1}. The absence of a very strong peak at 1544 cm^{-1} for NH_2 bending [33–36], indicates the successful grafting of chiral 4-oxazolinyl aniline ligands **8** onto the surface of MCM-41 (Fig. 1). The FT-IR spectra of the chiral catalyst OX-Ph-MCM-41 **9a** are presented in Fig. 1.

The organic content was investigated using TGA measurements of the samples Cl-MCM-41 and OX-R-MCM-41. As shown in Fig. 2, the weight loss of the samples in the temperature range 150–500 °C was 10.6 wt% and 15.64 wt% for Cl-MCM-41 and OX-R-MCM-41, respectively. All samples showed a weight loss of 1–2 wt% at temperatures lower than 150 °C, corresponding to desorption of physically adsorbed water. The DTA analysis data of samples showed a two-step weight loss at 370 and 500 °C due to the decomposition of propylaniline oxazoline from the surface of silanols. These data confirmed the covalent attachment of oxazolinyl aniline to MCM-41 (Fig. 2). TAG analysis of Cl-MCM-41 shows that the chlorine loading in the grafted material was 15/64% or 1.95 mmol chlorine/g of SiO_2. TGA analysis shows that the oxazoline loading in chiral catalyst OX-R-MCM-41 was in the range of 0.19–0.45 mmol oxazoline/g SiO_2 (Table 1).

Table 1
Density of grafted oxazoline, based on wt% N and weight loss in thermogravimetric traces.

Entry	Catalyst	Wt% change	Oxazoline grafted groups (base on CHN analyst) mmol oxazoline/g SiO_2	$\dot{\nu}$ C=N (FT-IR)
1	**9a**	10.7	0.45	1708
2	**9b**	4.8	0.19	1678
3	**9c**	3.9	0.19	1694
4	**9d**	6.2	0.28	1682

3.3.2. Textural properties of the chiral catalyst OX-R-MCM-41 ***9a–9d***

The XRD patterns of the MCM-41 and the chiral catalyst OX-R-MCM-41 are presented in Fig. 3. The XRD patterns of MCM-41 show four reflections (a very intense peak (100) and three additional high-order peaks (110), (200), and (210) with lower intensities). This result is characteristic of hexagonal pore structures. The (100) reflection of OX-R-MCM-41 with decreased intensity was retained after functionalization, while the (110), (200), and (210) reflections became weak and diffuse, which could be due to contrast matching between the silica framework and organic moieties that are located inside the mesoporous channels of MCM-41.

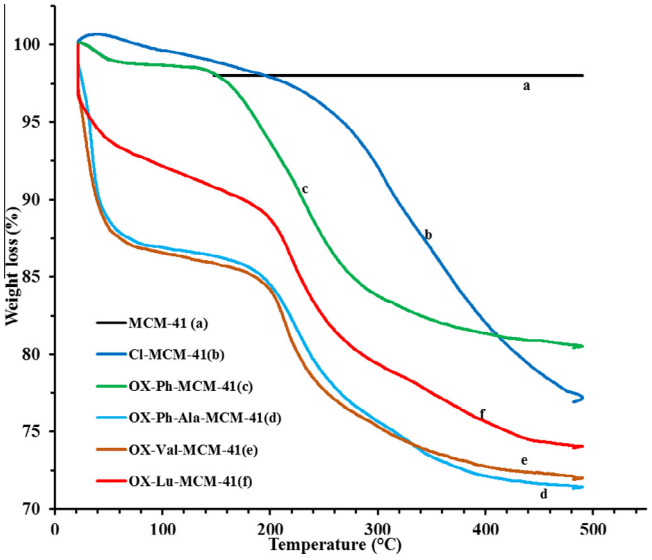

Fig. 2. Thermo gravimetric analysis (TGA) of OX-R-MCM-41, Cl-MCM-41 and MCM-41.

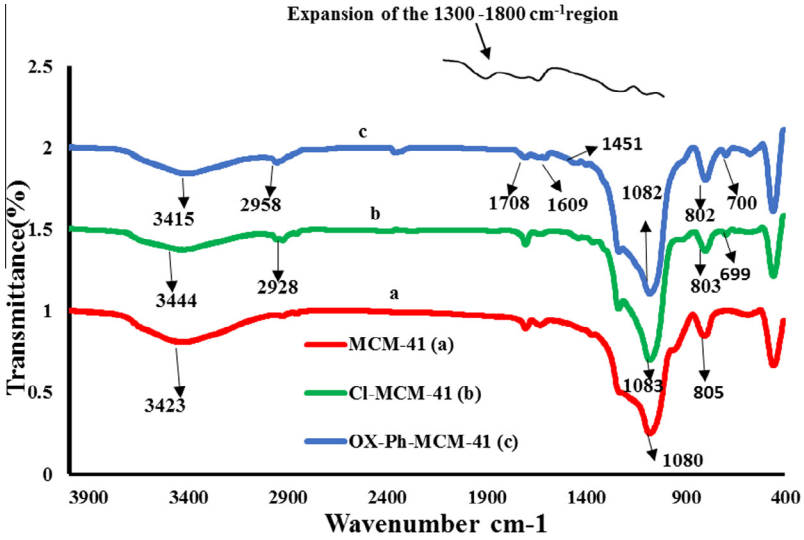

Fig. 1. FT-IR spectra of MCM-41, Cl-MCM-41, OX-Ph-MCM-41.

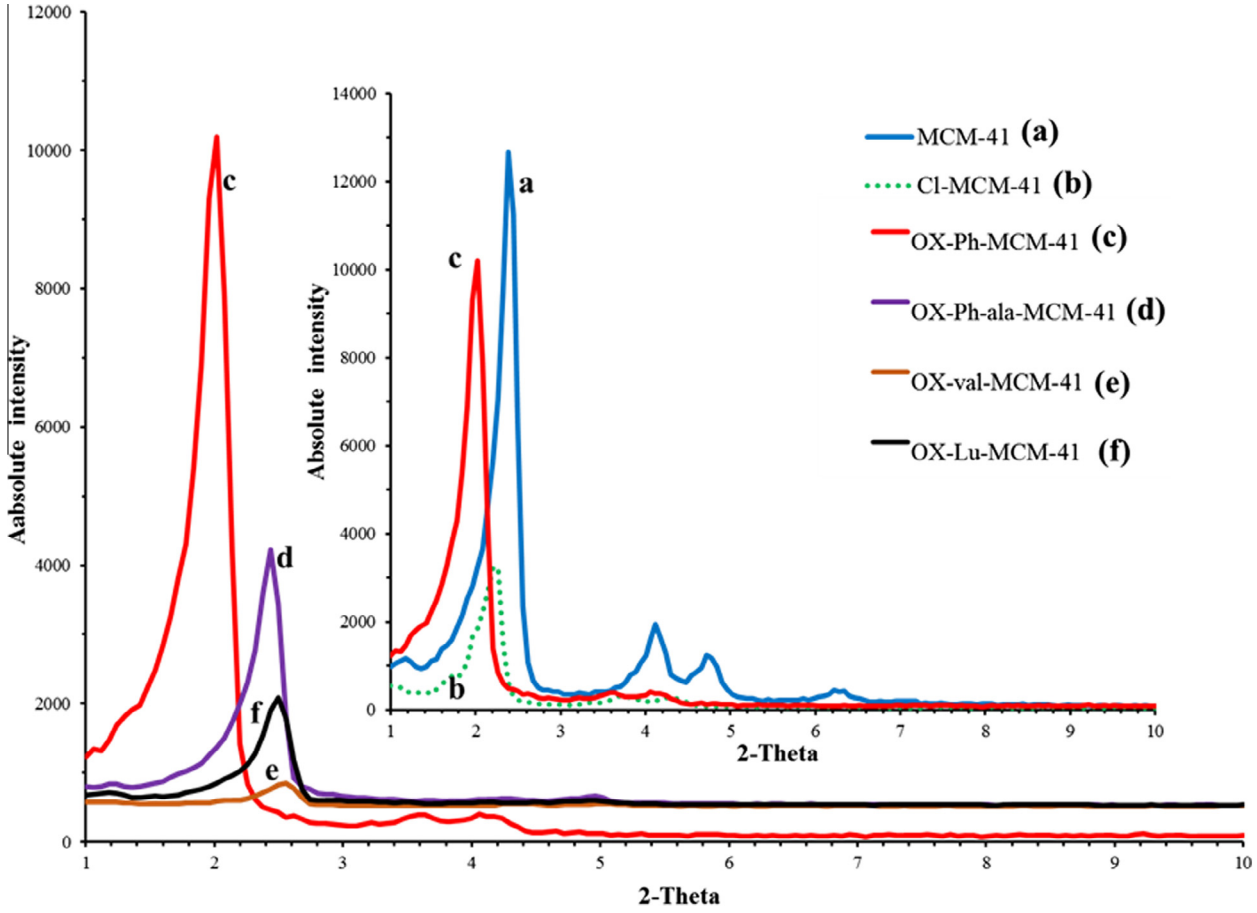

Fig. 3. XRD patterns of the parent MCM-41, Cl-MCM-41 and OX-R-MCM-41.

Table 2
Textural properties of different supports.

Sample	d_{100} (nm)[a]	a_0 (nm)[b]	BET surface area (m^2/g)	BET total pore volume (cm^3/g)	Average pore diameter (nm)	BJH pore volume (cm^3/g)	WTH (Å)[c]
MCM-41	4.1	4.8	1275	1.25	3.87	0.93	8.9
Cl-MCM-41	4.7	5.4	596	0.449	3.02	0.42	23.8
OX-Ph-MCM-41	4.9	5.7	210	0.195	3.71	0.155	17.2

[a] $\lambda = 2d_{100} \sin\theta$ (λ = 1.54060 Cu).
[b] Unit cell parameter: $a_0 = 2d_{100}/\sqrt{3}$.
[c] Wall thicknesses were calculated as a_0 – pore size.

In other words, the attachment of the organic functional groups onto the surface of the mesoporous channels tends to reduce the scattering power (or scattering contrast) of the silicate wall.

N_2 adsorption–desorption is a common method of characterizing mesoporous materials. This method provides information such as the specific surface area, average pore diameter, and pore volume. BET surface area, pore size, and pore volume for MCM-41 and the chiral catalyst OX-Ph-MCM-41 are presented in Table 2. MCM-41 has more surface area than OX-Ph-MCM-41. In other words, the surface area of MCM-41 decreased significantly with an increase in 4-oxazolinyl aniline content, which may be attributed to pore blocking due to overloading with oxazoline. The pore volume of MCM-41 showed the same trend as that of surface area, while the average pore diameter of OX-Ph-MCM-41 is slightly higher than that of Cl-MCM-41 (Table 2).

Combining the results from XRD and N_2 adsorption–desorption, the thickness of the silicate wall of OX-Ph-MCM-41 is 17.2 Å (Table 2).

The N_2 adsorption–desorption isotherms of the functionalized mesoporous silica are shown in Fig. 4a. The isotherm of OX-R-MCM-41 (**9a**–**9d**) is classified as type IV, characteristic of mesoporous materials [33–37]. A linear increase of adsorbed volume at low pressure followed by a noticeable increase in the adsorbed volume of N_2 and finally by a slow increase at high pressure is observed. The adsorption at low relative pressure P/P_0 occurs from the monolayer adsorption of N_2 onto the walls of the mesopores and it does not represent the presence of any micropores. The inflection about $P/P_0 = 0.1$ in the adsorption isotherm of OX-Ph-MCM-41 suggests the filling of the mesopore system. N_2 adsorption in the mesopore region is saturated at about $P/P_0 = 0.3$. Larger pores are filled at higher P/P_0.

Morphological changes were investigated by scanning electron microscopy (SEM) of MCM-41, Cl-MCM-41 (S44-S46 in the Supplementary Material), and OX-Ph-MCM-41 (Fig. 4b). The EDX spectrum shows the elemental composition of OX-Ph-MCM-4 (Fig. 4c).

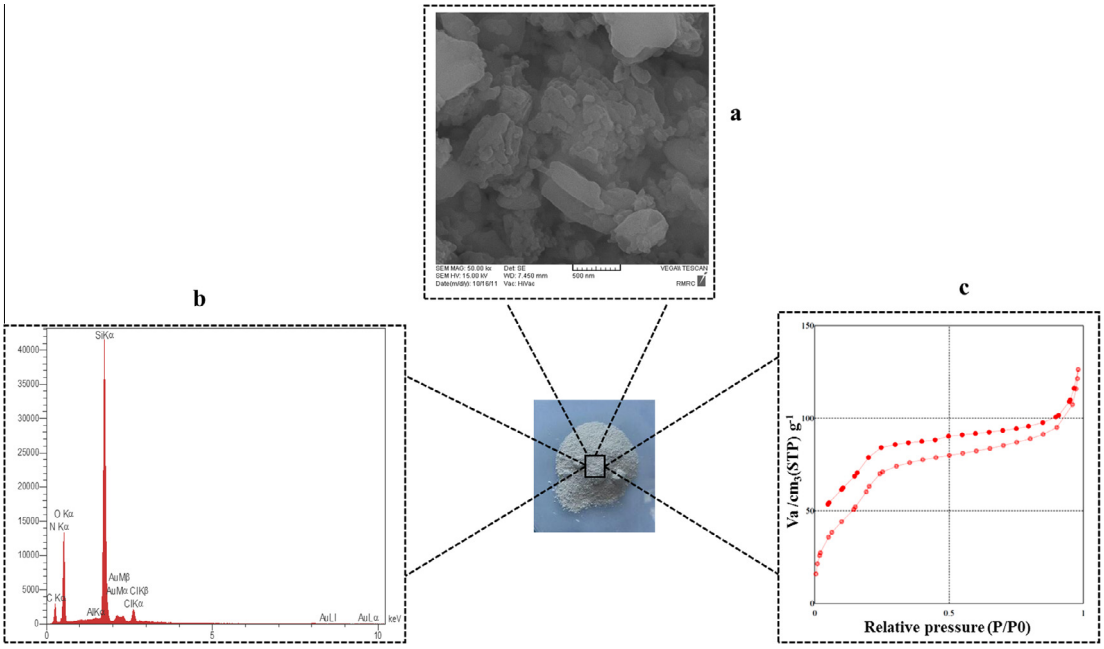

Fig. 4. (a) N_2 adsorption–desorption isotherm of chiral OX-Ph-MCM-41 at 77 K. b). Scanning electron micrographs of OX-Ph-MCM-41. c). EDX spectrum of the OX-Ph-MCM-41.

Table 3
Effects of heterogeneous catalysts **9a**–**d** on reaction at different temperatures.

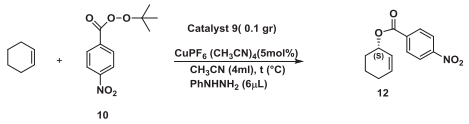

Entry	Catalyst	Temperature (°C)	Time (h)	Yield (%)	ee (%)
1	**9a**	25	3.5	95	38
2	**9a**	10	24	93	52
3	**9a**	0	82	85	54
4	**9a**	−10	195	82	70
5[a]	**9a**	−10	456	60	65
6	**9b**	−10	185	82	60
7	**9c**	−10	195	70	33
8	**9d**	−10	186	75	33
9	**8a**	−10	150	30	20

[a] In the absence of phenylhydrazine.

Table 4
Effects of catalyst loading on reaction.

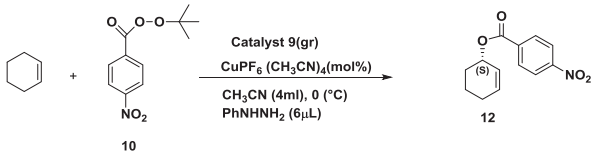

Entry	$CuPF_6$ (mol%)	Catalyst (g)	Time (h)	Yield (%)	ee (%)
1	5	0.1	195	82	70
2	5	0.05	340	63	53
3	5	0.15	185	82	35
3	5	0.025	220	40	25
5	10	0.1	175	65	45
6	2.5	0.1	>400	25	37

3.4. Catalytic and induced asymmetric effects of the chiral copper (I) complexes of OX-R-MCM-41 in the enantioselective Kharash–Sosnovsky reaction

3.4.1. Optimization of the model reaction

In order to evaluate the potential of the new heterogeneous catalyst **9** in the catalytic asymmetric reaction, its application in the copper-catalyzed allylic oxidation of cycloolefins was investigated. In a typical experimental procedure, the reactions were carried out using cyclohexene (5 mmol) as the substrate and *tert*-butyl 4-nitrobenzoperoxoate (0.85 mmol) **10** as an oxidant in the presence of various heterogeneous catalysts **9a**–**9d** (0.1 g) and [Cu $(CH_3CN)_4$] PF_6 (5 mol%) at different temperatures in acetonitrile. The reactions were monitored by TLC for consumption of the perester and stopped at the given time [14,24]. The obtained results are summarized in Table 3.

Temperature dependence of yields and enantiomeric excess of products was observed. A decrease in the reaction temperature from 25 to −10 °C leads to a favorable ee% and greatly decreases the reaction yield and reactivity (entries 1–4). Further reduction of the reaction temperature results in a decrease in reactivity and yield without any significant increase in enantioselectivity.

The effect of phenylhydrazine was also investigated. It was observed that in the absence of phenylhydrazine, enantioselectivity and yield only slightly decrease but reaction rate drops considerably (entry 5). In fact, phenylhydrazine acts as a reducing agent to regenerate Cu(I) in the catalytic cycle [14,27].

The phenyl- or benzyl-substituted oxazolines in catalysts **9a** and **9b** resulted in considerably higher enantioselectivities than the other two catalysts **9c** and **9d** carrying alkyl substitutions (entries 4 and 6 vs. 7 and 8). The highest enantioselectivity was achieved by employing catalyst **9a** in −10 °C (entry 4, Table 3).

For comparison, in the reaction carried out under the homogeneous catalytic influence of chiral 4-oxazolinyl aniline ligands **8a**, low yield (30%) and enantiomeric excess (20%) of the desired product were obtained after 150 h (Table 3, entry 9). Therefore, the remarkable efficiency of OX-R-MCM-41 can be explained by the existence of multiple catalytic centers (Table 3, entries 1–8).

Table 5
Synthesis of allylic esters **11**–**15** by allylic oxidation of various cycloolefins over OX-R-MCM-41 catalyst.

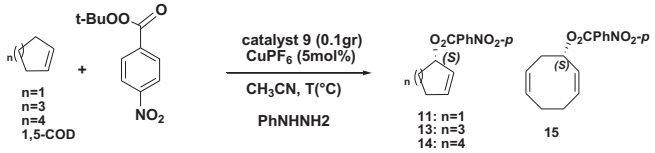

Catalyst	**11**			**13**			**14**			**15**		
	Time (h)	Yield (%)	ee (%)	Time (h)	Yield (%)	ee (%)	Time (h)	Yield (%)	ee (%)	Time (h)	Yield (%)	ee (%)
9a	150	70	53	175	75	50	250	59	53	140	95	80
9b	185	62	48	215	55	57	255	59	50	180	85	68
9c	250	65	22	225	50	28	280	55	18	210	75	32
9d	235	60	15	225	55	20	300	45	10	225	80	23

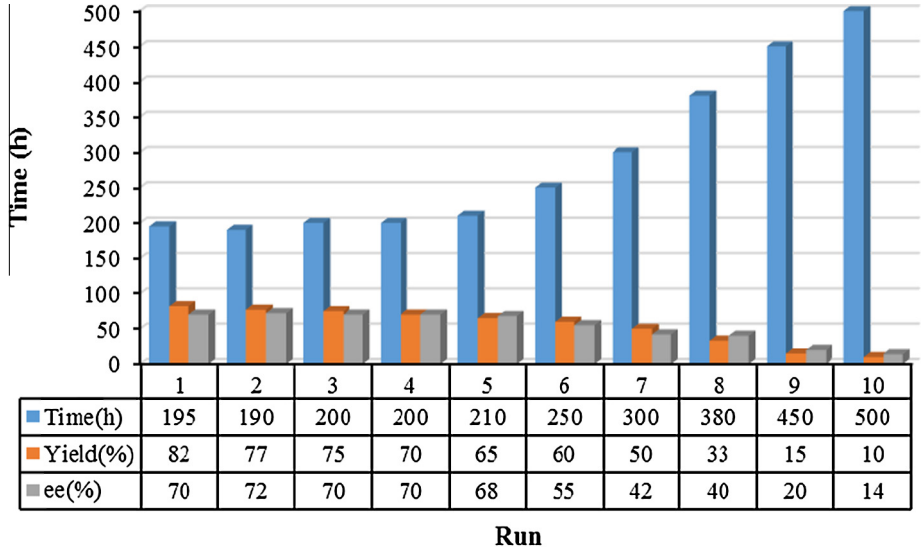

Fig. 5. Correlation between recyclability of OX-Ph-MCM-41 and time, yield, and ee%.

The effects of catalyst loading were also investigated. The results described in Table 4 indicate that the enantioselectivity, reactivity, and yield are influenced by the amount of this catalyst. The best result was achieved when the amount of OX-Ph-MCM-41 was 0.1 g of catalyst containing 0.045 mmol of oxazoline per 5 mmol of substrate (cyclohexene) and the amount of $CuPF_6$ was 5% mmol (entry 1, Table 4) [14,24].

3.4.2. Evaluation of the scope of the reaction

To expand the generality of this novel catalytic method, various cycloolefins were tested under the optimized conditions and the results are presented in Table 5. In the case of 1,5-cycloocadiene in the presence of catalyst **9a**, the reaction was carried out at a higher rate and yield and attained the highest enantiomeric excess (80%) in comparison with other cycloolefins.

3.5. Recycling of the catalyst

The reusability of the chiral heterogeneous catalyst **9a** (OX-Ph-MCM-41) was also examined. As shown in Fig. 5, the catalyst was recycled for subsequent runs. It was found that the catalyst is still active even in fifth runs, with a gradual decrease in activity, while moderate to good enantioselectivity is still observed. The XRD, SEM, and IR results clearly demonstrate that the mesoporous structure of catalyst **9a** was preserved after 10 times recycling. The recovery of the catalyst was very easy. The catalyst was simply filtered from the resulting mixture, dried at 40 °C for 4 h under vacuum, and reused in subsequent runs. No fresh catalyst was added.

*3.6. Proposed mechanism for the model reaction in the presence of the chiral heterogeneous catalysts **9a**–**9d***

A mechanistic rationalization for asymmetric allylic oxidation of cyclohexene in the present of the chiral heterogeneous catalysts **9a**–**9d** is shown in Scheme 4. The Cu(I) species cleaves the oxygen–oxygen bond in *tert*-butyl 4-nitrobenzoperoxoate to form Cu(II) benzoate and *tert*-butoxy radicals. The *tert*-butoxy radical abstracts a prochiral hydrogen atom from the allylic position of the olefin to give *tert*-butyl alcohol and allylic radicals. The allylic radicals add to the Cu(II) benzoate to generate Cu(III) benzoate, which can rearrange via a six-membered cyclic transition state to give allylic benzoate and regenerated Cu(I) catalyst [38]. Fortunately, the Cu(III)

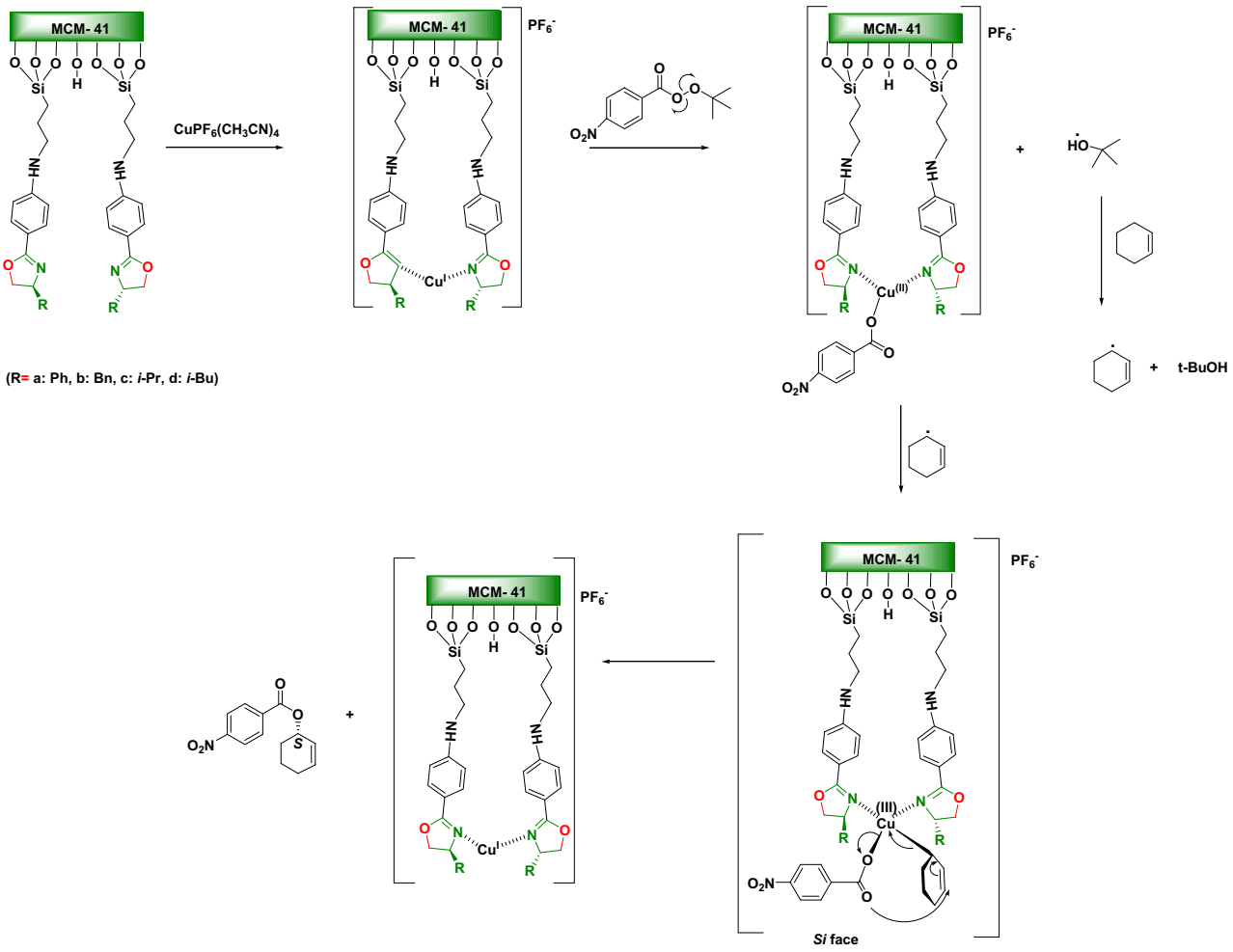

Scheme 4. Proposed pathway for asymmetric allylic oxidation of cyclohexene in the present of chiral heterogeneous catalysts **9a**–**9d**.

intermediate has been detected by rapid injection NMR (RI-NMR) [39].

4. Conclusions

A new class of supported heterogeneous catalysts has been synthesized through the reaction of chloropropyl modified MCM-41 with different chiral amino oxazoline ligands, which were successfully synthesized by a simple method. The heterogenized catalysts showed moderate to good enantioselectivities, up to 80%, and good yields, up to 95% better than the corresponding homogeneous reaction and exhibited good recyclability.

Acknowledgments

We are grateful to the University of Kurdistan Research Councils and the Research Council of Shahid Beheshti University for partial support of this work.

Appendix A. Supplementary material

Supplementary data (including IR, mass, ^{1}H, and ^{13}C spectra for compounds, chromatograms and TGA-DTA analysis, SEM, DEX, X-ray scattering, and typical procedure for the synthesis of compounds **2**, **10**–**15**, MCM-41, Cl-MCM-41). Supplementary data associated with this article can be found, in the online version, at http://dx.doi.org/10.1016/j.jcat.2016.05.021.

References

[1] D.E. De Vos, M. Dams, B.F. Sels, P.A. Jacobs, Chem. Rev. 102 (2002) 3615–3640.
[2] C.E. Song, S.-G. Lee, Chem. Rev. 102 (2002) 3495–3524.
[3] B.J. Pugin, Mol. Catal. A Chem. 107 (1996) 273–279.
[4] Q.-H. Fan, Y.-M. Li, A.S.C. Chan, Chem. Rev. 102 (2002) 3385–3465.
[5] S. Taylor, J. Gullick, P. McMorn, D. Bethell, P.C.B. Page, F.E. Hancock, F. King, G.J. Hutchings, J. Chem. Soc. Perkin Trans. 2 (2001) 1714–1723.
[6] S. Taylor, J. Gullick, P. McMorn, D. Bethell, P.C.B. Page, F.E. Hancock, F. King, G.J. Hutchings, J. Chem. Soc. Perkin Trans. 2 (2001) 1724–1728.
[7] M. Benaglia (Ed.), Recoverable and Recyclable Catalysts, John Wiley & Sons, 2009.
[8] M. Pagliaro, Silica-based Materials for Advanced Chemical Applications, RSC Publishing, 2009.
[9] C.E. Song, S.G. Lee, Chem. Rev. 102 (2002) 3495.
[10] J.M. Fraile, J.I. García, J.A. Mayoral, E. Pires, Heterogenization on inorganic supports: methods and applications, in: P. Barbaro, F. Liguori (Eds.), Heterogenized Homogeneous Catalysts for Fine Chemicals Production, Springer Science+Business Media, 2010.
[11] Z. Yang, Y. Lu, Z. Yang, Chem. Commun. (2009) 2270.
[12] R.I. Kureshy, I. Ahmad, N.H. Khan, S.H.R. Abdi, K. Pathak, R.V. Jasra, J. Catal. 238 (2006) 134.
[13] C. Li, H. Zhang, D. Jiang, Q. Yang, Chem. Commun. 547 (2007).
[14] S. Samadi, K. Jadidi, B. Notash, Tetrahedron Asymmetry 24 (2013) 269–277.
[15] S. Samadi, S. Nazari, H. Arvinnezhad, K. Jadidi, B. Notash, Tetrahedron 69 (2013) 6679–6686.
[16] L. Faraji, S. Samadi, K. Jadidi, B. Notash, Bull. Korean Chem. Soc. 35 (2014) 1989–1995.
[17] P. Braunstein, F. Naud, Angew. Chem. Int. Ed. 40 (2001) 680 (Angew. Chem. 113 (2001) 702).
[18] F. Fache, E. Schulz, M.L. Tommasino, M. Lemaire, Chem. Rev. 100 (2000) 2159.

[19] O.B. Sutcliffe, M.R. Bryce, Tetrahedron Asymmetry 14 (2003) 2297.
[20] L.H. Gade, S. Bellemin-Laponnaz, Coord. Chem. Rev. 251 (2007) 718.
[21] T.G. Kilroy, P.G. Cozzi, N. End, P.J. Guiry, Synlett 11 (2004) 1879.
[22] G. Desimoni, G. Faita, K.A. Jørgensen, Chem. Rev. 106 (2006) 3561.
[23] M.B. Andrus, D. Asgari, Tetrahedron 56 (2000) 5775.
[24] M.B. Andrus, Z. Zhou, J. Am. Chem. Soc. 124 (2002) 8806.
[25] J. Bayardon, D. Sinou, M. Guala, G. Desimoni, Tetrahedron Asymmetry 15 (2004) 3195.
[26] J.S. Clark, M.R. Clarke, J. Clough, A.J. Blake, C. Wilson, Tetrahedron Lett. 45 (2004) 9447.
[27] V.K. Singh, A. Dattagupta, S. Govindasamy, J. Org. Chem. 63 (1998) 2961–2967.
[28] S.K. Ginotra, V.K. Singh, Org. Biomol. Chem. 4 (2006) 4370.
[29] Q. Tan, M. Hayashi, Org. Lett. 11 (2009) 3314.
[30] F. Mu, S.L. Coffing, D.J. Riese II, R.L. Geahlen, P. Verdier-Pinnard, E. Hamel, J. Johnson, M. Cushman, J. Med. Chem. 44 (2001) 441.
[31] M.J. McKennon, A.I. Meyers, J. Org. Chem. 58 (1993) 3868.
[32] D. Kumar, K. Schumacher, M. Grun, K.K. Unger, Colloids Surf. 187 (2001) 109.
[33] J.C. Vartuli, K.D. Schmitt, C.T. Kresge, W.J. Rout, M.E. Leonowicz, S.B. McCullen, S.D. Hellering, J.L. Beck, D.H. Olson, E.W. Sheppard, Chem. Mater. 6 (1994) 2317.
[34] C.D. Nunes, A.A. Valente, M. Pillinger, A.C. Fernandes, C.C. Romão, J. Rocha, I.S. Gonçalves, J. Mater. Chem. 12 (2002) 1735.
[35] C. Lesaint, B. Lebeau, C. Marichal, J. Patarin, Micropor. Mesopor. Mater. 83 (2005) 76.
[36] D. Kumar, K. Schumacher, C. du Fresne von Hohenesche, M. Grün, K.K. Unger, Colloids Surf. A 187 (2001) 109.
[37] L. Bois, A. Bonhomme, A. Ribes, B. Pais, G. Raffin, F. Tessier, Colloids Surf. A 221 (2003) 221.
[38] J.A. Mayoral, S. Rodríguez-Rodríguez, L. Salvatella, Chem. Eur. J. 14 (2008) 9274–9284.
[39] S.H. Bertz, S. Cope, M. Murphy, C.A. Ogle, B.J. Taylor, J. Am. Chem. Soc. 129 (2007) 7208–7209.